DESY 11-149
SHEP-11-24

Indirect Evidence for New Physics at the 10 TeV Scale

H. Kowalski [1], L.N. Lipatov [2], and D.A. Ross [3]

[1] *Deutsches Elektronen-Synchrotron DESY, D-22607 Hamburg, Germany*

[2] *Petersburg Nuclear Physics Institute, Gatchina 188300, St. Petersburg, Russia*

[3] *School of Physics and Astronomy, University of Southampton, Highfield, Southampton SO17 1BJ, UK*

Abstract

We show that the supersymmetric extension of the Standard Model modifies the structure of the low lying BFKL discrete pomeron states (DPS) which give a sizable contribution to the gluon structure function in the HERA x and Q^2 region. The comparison of the gluon density, determined within DPS with N=1 SUSY, with data favours a supersymmetry scale of the order of 10 TeV. The DPS method described here could open a new window to the physics beyond the Standard Model.

September 2011

1 Introduction

In our previous paper [1] we have shown that HERA F_2 data, at low x, can be very well described by the gluon density constructed from the discrete spectrum of eigenfunctions of the BFKL kernel, i.e. from the pomeron wave functions. This first successful confrontation of the BFKL formalism [3] with data led to the unexpected question as to whether the HERA data are sensitive to the Beyond Standard Model (BSM) effects. These effects, although only present at scales that are much higher than the region of HERA data, can nevertheless affect the quality of the fits to data because the shape of many of the contributing eigenfunctions has an apparent sensitivity to the BSM effects. This apparent sensitivity is due to the fact that the support of eigenfunctions extends to very high transverse momenta where BSM effects have to be present. Since the eigenfunctions are constructed in a global way, i.e. the behaviour of the eigenfunctions at energies way above the threshold feeds into their behaviour at low energies, these eigenfunctions will be sensitive to any BSM physics.

In this paper we investigate whether this possible sensitivity to BSM effects indeed exist, as it also depends on an adequate treatment of the infrared boundary condition. As a popular example of BSM effects we have chosen the N=1 supersymmetry. For this purpose we modified the beta function and the kernel of the BFKL equation to include the contributions from the superpartners and confronted the modified gluon density with data.

The paper is organized as follows; in Section 2 we give a brief summary of the properties of the discrete pomeron solution to the BFKL equation. In Section 3 we describe the construction of the infrared boundary condition and the changes introduced by the two-loop running of the coupling. In Section 4 we discuss the effects of the supersymmetric changes of the β-function and of the eigenfunctions of the BFKL kernel. In Section 5 we present and discuss the results and in Section 6 we describe the properties of the determined infrared boundary. In Section 7 we give a summary.

2 The Discrete Pomeron Solution to the BFKL Equation

In this section we give a brief summary of the properties of the discrete pomeron solution to the BFKL equation, described in detail in [1].

The BFKL amplitude for the scattering of high-energy gluons with transverse momenta $\mathbf{k}$ and $\mathbf{k}'$, is a Green function constructed from the discrete eigenfunctions of the BFKL kernel, i.e. the solutions $f_n(k)$ to the equation

$$\int d^2\mathbf{k}' \mathcal{K}\left(\mathbf{k}, \mathbf{k}', \alpha_s(k^2)\right) f_n(\mathbf{k}') \;=\; \omega_n f_n(\mathbf{k}'). \tag{2.1}$$

where $\alpha_s(k^2)$ is the strong coupling which runs with the magnitude, k, of the transverse momentum of one of the gluons. This running leads to an oscillatory eigenfunction, f_n, whose frequency, ν_n, in the semiclassical approximation, depends on the transverse momentum, k,

so that the eigenvalues, ω_n, are given in terms of the LO and NLO characteristic functions of the oscillation frequency ν,

$$\omega \;=\; \left(\frac{\alpha_s(k^2)C_A}{\pi}\right)\chi_0(\nu) + \left(\frac{\alpha_s(k^2)C_A}{\pi}\right)^2\chi_1(\nu) + \cdots, \tag{2.2}$$

where for the moment we have ignored the resummation of collinear divergences in the NLO characteristic function [5]. The frequency depends on ω and decreases as k increases, reaching a critical point k_{crit} at $\nu(k_{crit}) = 0$ where it changes from real to imaginary values. Below k_{crit} the eigenfunction has an oscillatory behaviour but above k_{crit} it decreases exponentially with $\ln k$. The matching of the phases immediately below and above the critical point fixes the phase of the oscillations at k_{crit} to be $-\pi/4$ (this being the phase of the Airy function, which was shown in ref. [1,6,7] to provide a very good approximation to the eigenfunctions). This phase, $\phi(k)$, at any lower value of k is then determined by integrating the k-dependent frequency from k_{crit} to k, namely

$$\phi(k) \;=\; -\frac{\pi}{4} + 2\int_k^{k_{crit}} \nu(k) d\ln(k). \tag{2.3}$$

For a given value of ω the phase, $\eta\,\pi$, of the oscillation at some infrared transverse momentum, k_0, is determined from the perturbative BFKL dynamics (with running coupling), through eqs.(2.1,2.2). We make a very general assumption that the infrared (non-perturbative) properties of QCD impose some phase at k_0, defined up to an ambiguity of $n\pi$, which can also depend on ω. We find then that we can only match this phase to that determined from eq.(2.3) for one value of ω, for each integer n, where n corresponds to the number of turning points of the eigenfunctions. This leads to the quantization of the spectrum (i.e. discrete pomeron poles), in keeping with the predictions of Regge theory.

Before a comparison can be made with the measured structure function, F_2, it is necessary to convolute this Green function with the impact factors for the virtual photon at one end and for the proton at the other, (see Section 6 of ref. [1]). The impact factor for the virtual photon is calculable in perturbative QCD and has support, which is peaked at transverse momenta of the order of the Q^2 argument of the structure function, whereas the proton impact factor cannot be so calculated and is assumed to have a simple form with support up to $\mathcal{O}(1)$ GeV.

One of the main results of ref. [1] was that a very good quality fit to HERA-F_2 data [2] (with Q^2 above $8\,\mathrm{GeV}^2$) is obtained taking a very simple form for the dependence of the above-mentioned (non-perturbative) infrared phase, η_n, on eigenfunction index n. It was found that in order to obtain this good description of data, it was necessary to take around 120 eigenfunctions of the BFKL kernel.

Although the oscillation frequency varies with transverse momentum, k, the period, Δ, of oscillation (in $\ln(k)$) defined by

$$2\int_{\ln(k)}^{\ln(k)+\Delta} \nu(k') d\ln(k') \;=\; 2\pi \tag{2.4}$$

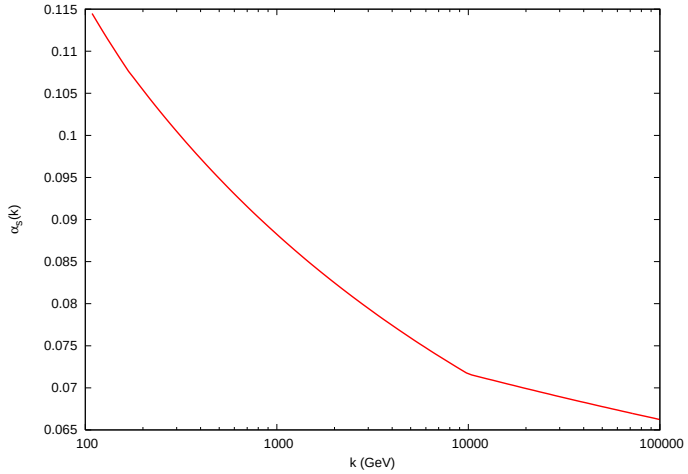

Figure 1: The running of α_s across a threshold for N=1 SUSY at 10 TeV

turns out to be roughly constant ($\Delta \sim 8$), beyond the first two turning points. This means that the main difference between the n^{th} and $(n+1)^{th}$ (for $n > 2$) eigenfunction is that the latter has one more half period, which leads to a rapid increase in the critical momentum, k_{crit} with eigenfunction index n

$$k_{crit} \sim c \cdot e^{4n}, \tag{2.5}$$

where c is a constant of the order of Λ_{QCD}. For the first eigenfunction the value of k_{crit} is $\mathcal{O}(10\,\text{GeV})$. It therefore follows that k_{crit} rapidly exceeds the threshold for most postulated theories beyond the Standard Model. On the other hand, if a threshold for new physics does indeed exist, the oscillation frequency is affected above this threshold and consequently the oscillation phase at *all* lower transverse momenta will be altered thereby affecting the matching of the phase to the phase imposed by the infrared dynamics of QCD. This in turn modifies the pomeron spectrum, ω_n. It is in this sense that a modification of the high-energy behaviour of the eigenfunctions "feeds" into the low-energy behaviour.

This immediately posed the question as to what the effects would be on the quality of the fit, if there were some new physics far above the energy scale of HERA.

3 The Infrared Boundary

In ref. [1], we defined the infrared boundary as a phase condition at the lowest possible value of the transverse momentum, $k = k_0$, which can be safely reached by the perturbative calculation. To make this value as close as possible to Λ_{QCD} we considered only the one-loop running of the coupling. This gave a value of $k_0 = 0.3$ GeV, which corresponds to $\alpha_s \sim 0.7$. The reason for running the coupling at one-loop only was that in principle this is the same order of perturbation theory as the NLO characteristic function, χ_1 [4].

However, given that we modify eq.(2.1) by resumming all the large corrections in χ_1 using the technique of ref. [5], it is more appropriate to take the β-function to two-loop order which is what we use in this paper.

When we do this, we are faced with a problem - namely that we cannot run the coupling below an "infrared" scale $k_0 = 0.6$ GeV, which corresponds to $\alpha_s \sim 0.7$ (at the two loop level), without approaching the Landau pole too closely. On the other hand, the infrared boundary conditions are to be imposed at a transverse momentum of order Λ_{QCD}. Moreover we need to know the eigenfunctions below k_0 in order to perform a convolution with the proton impact factor, which has support mainly below the k_0 value. Therefore, guided by the behaviour of the eigenfunctions in perturbative QCD, we continue them down to a lower momentum $\tilde{k}_0$, which should be of order Λ_{QCD}, using the extrapolation of the phase $\phi_n(k)$

$$\phi_n(\tilde{k}_0) \;=\; \phi_n(k_0) - 2\nu_n^0 \ln\left(\frac{k_0}{\tilde{k}_0}\right), \tag{3.1}$$

where for each eigenfunction, with index n, ν_n^0 is the frequency of the oscillations near $k = k_0$ [1]. We have assumed that this frequency is constant below k_0, an assumption which is correct for sufficiently small k_0, at least for the leading order BFKL kernel (see [7]). Any deviation from constant frequency should have a negligible effect as we are only extrapolating over a small range in gluon transverse momentum. The numerical values of ν_n^0 are obtained by inverting the eigenvalue equation (2.2), modified according to [5].

4 N=1 Supersymmetry at various Thresholds

The "new physics" that we investigate in this paper is the popular $N = 1$ supersymmetric extension of the Standard model above a given threshold k_T, which for simplicity we assume to be a common mass threshold for all superpartners. Below this threshold the running of the coupling is governed by the β-function to two-loop order

$$\beta_< \;=\; -\frac{\alpha_s^2}{4\pi}\left(\frac{11C_A}{3} - \frac{2}{3}n_f\right) - \frac{\alpha_s^3}{(4\pi)^2}\left(\frac{34C_A^2}{3} + \left(\frac{10C_A}{3} + 2C_F\right)n_f\right), \tag{4.1}$$

where for the case of QCD, $C_A = 3$, $C_F = 4/3$ and n_f is the number of active flavours. Above the threshold, the beta function is given by

$$\beta_> \;=\; -\frac{\alpha_s^2}{4\pi}\left(3C_A - n_f\right) - \frac{\alpha_s^3}{(4\pi)^2}\left(6C_A^2 + \left(-\frac{2C_A}{3} + 2C_F\right)n_f\right). \tag{4.2}$$

This leads to a "kink" (discontinuity in the derivative) in the running of α_s at the threshold for N=1 SUSY, which can be seen in Fig.1.

The fact that the coupling runs more slowly above the SUSY threshold means that the oscillation frequency varies more slowly with k and therefore the critical transverse momentum, k_{crit} (where $\nu = 0$), is pushed out further away. Thus, for example, in the case of a SUSY threshold at 10 TeV, if we assume that the phase of the oscillations is zero at $k_0 = 0.6$ GeV [1], the first two eigenfunctions are identical as the critical momentum

[1] This phase is merely an example designed to illustrate the difference in the behaviour of the eigenfunctions for the Standard model and the N=1 SUSY model. In practice these phases are determined from the fit to data and are different for the two models.

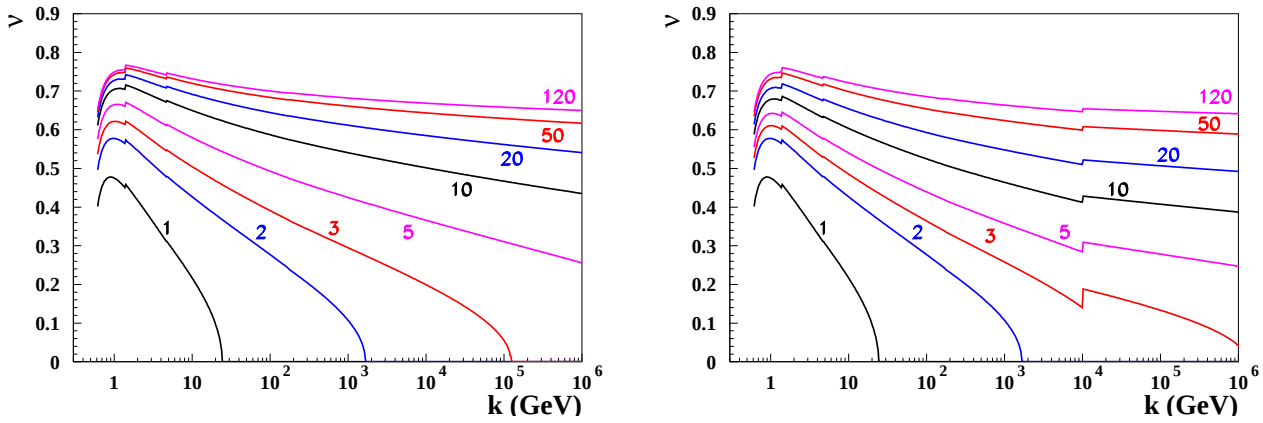

Figure 2: Oscillation frequencies as a function of gluon transverse momentum for various eigenfunctions. The left-hand pane is the case of the Standard Model and the right-hand pane is the case of N=1 SUSY above a threshold of 10 TeV. For the purpose of this comparison it has been assumed that the infrared phases are the same in both cases.

is below the threshold, whereas for the third eigenfunction the critical momentum is at $k_{crit} = 1.2 \times 10^5\, GeV$ in the case of the SM but at $k_{crit} = 1.3 \times 10^6\, GeV$ in the case of SUSY. This can be seen from Fig.2.

Furthermore the NLO characteristic function, $\chi_1(\nu)$ acquires an additional contribution [9] of

$$\delta_f \chi_1(\nu) \;=\; \frac{\pi^2}{32} \frac{\sinh(\pi\nu)}{\nu(1+\nu^2)\cosh^2(\pi\nu)} \left(\frac{11}{4} + 3\nu^2\right) \tag{4.3}$$

from the octet of Majorana fermions (gluinos), and

$$\delta_s \chi_1(\nu) \;=\; -\frac{\pi^2}{32} \frac{n_f}{C_A^3} \frac{\sinh(\pi\nu)}{\nu(1+\nu^2)\cosh^2(\pi\nu)} \left(\frac{5}{4} + \nu^2\right) \tag{4.4}$$

from the squarks. Note that it is this discontinuity in χ_1 at the SUSY threshold which is responsible for the discontinuities in the frequencies at threshold and *not* the change in the rate of running of the coupling, which remains a continuous function[2]. The change in frequency thus compensates for the change in the characteristic function in order to ensure that the eigenvalues, ω_n remain unchanged as one passes through the threshold [3].

The contribution, $\delta\chi_1$, of these additional terms to χ_1 is shown as a function of frequency in Fig. 3 where it can be seen that this is a rapidly decreasing function, which explains why the discontinuities in frequency at threshold are much larger for the lower eigenfunctions for which the frequency at threshold is lower.

[2] A similar smaller discontinuity can be seen at around 3 GeV. This corresponds to the c-quark threshold. There are analogous, even smaller, discontinuities at the b-quark and t-quarks thresholds

[3] The discontinuous changes in frequency are due to the fact that the change in characteristic function is imposed at a threshold in its entirety. A determination of the NLO characteristic function which accounted for the mass of internal particles would smooth out these discontinuities.

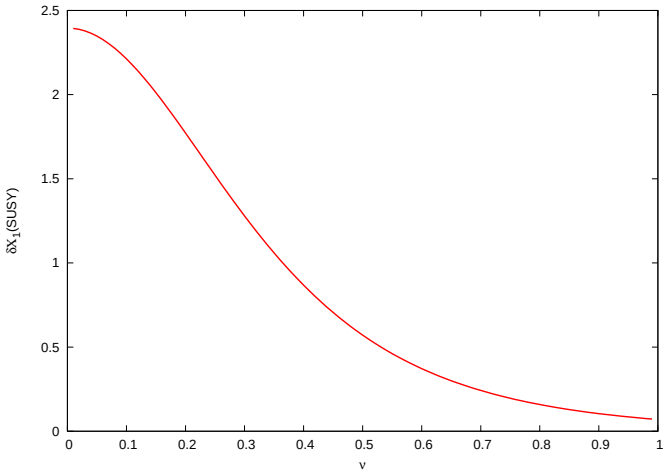

Figure 3: Increase in the NLO characteristic function, χ_1 as a function of frequency ν

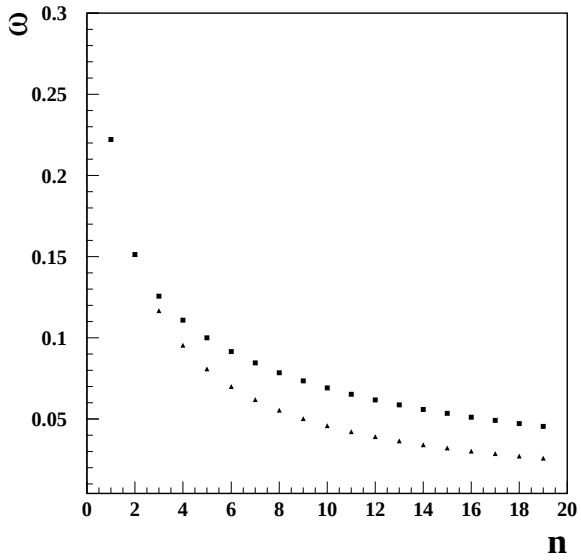

Figure 4: The first 20 eigenvalues in the case of the Standard model (triangles) and SUSY at a threshold of 10 TeV (squares)

The differences in frequencies also affect the magnitude of the eigenvalues, beyond the first two, as can be seen in Fig. 4. The simplest way to understand this is to consider the value of α_s at k_{crit} for the two models. Although k_{crit} is an order of magnitude larger for the SUSY model, the fact that the coupling runs more slowly actually means that the value of the coupling at k_{crit} is slightly *larger* for the SUSY model. Moreover the NLO characteristic function is larger in the SUSY model. These two effects combine to produce somewhat larger eigenvalues - in the case of the third eigenvalue the difference is about 0.01. For the higher eigenfunctions, for which k_{crit} is sufficiently large, eq.(2.2) is a valid approximation (at k_{crit}) without collinear resummation, we may approximate the difference, $\delta\omega_{12}$, in eigenvalue between the two models in terms of the difference of the running couplings, $\alpha_s(k_{crit\,1}) - \alpha_s(k_{crit\,2})$, at the value of k_{crit} for each model (where the frequency vanishes), namely

$$\delta\omega_{12} \;\approx\; (\alpha_s(k_{crit\,1}) - \alpha_s(k_{crit\,2}))\,\frac{C_A}{\pi}\chi_0(0) + \left(\frac{\alpha_s(k_{crit\,1})C_A}{\pi}\right)^2 \delta\chi_1(0), \tag{4.5}$$

which gives numerical results in agreement with those seen in Fig. 4 for $n > 10$.

In Fig. 5 we show a representative subset of eigenfunctions in the Standard Model and the SUSY model in the transverse momentum region relevant for a fit to HERA data. The eigenfunctions are computed at the same value of $\eta = 0$ to display SUSY effects only (in the fit the eigenfunctions with the same n have in general somewhat different η's). As expected, the first two eigenfunctions are identical since their values of k_{crit} are below the SUSY threshold. The third and higher eigenfunctions display significant differences which affect the quality of the fits to data. Remarkably, these differences diminish for higher eigenfunctions and for $n = 41$ the two eigenfunctions almost overlap in this region. The reason for this can be seen from Fig. 2, which shows that for the relatively low transverse momenta the differences in the frequencies between the two models decreases with increasing eigenvalue number, so that if the infrared phases are equal, the functions will be almost identical in this region.

5 Results

One of the main results of the previous paper [1] was that we found a simple power dependence between the infrared phase $\eta_n(k_0)$ and the eigenfunction number n. In this paper we use the same functional dependence, defined for $\eta_n(\tilde{k}_0)$, where $\tilde{k}_0$ denotes an infrared scale at which the phase of the leading eigenfunction vanishes. The relation between the η phase at $\tilde{k}_0$ and k_0 is given by eq.(3.1), where the value of $\tilde{k}_0$ should be close to Λ_{QCD}. Thus we take the parameterization

$$\eta_n(\tilde{k}_0) \;=\; \eta_0 \left(\frac{(n-1)}{(n_{max}-1)}\right)^{\kappa}, \tag{5.1}$$

where n_{max} is the number of eigenfunctions we use for the fit and η_0 represents the total range (in units of π) of infrared phases that are used for the fit. The value of the parameters $\tilde{k}_0$, κ and η_0 are determined in the fit.

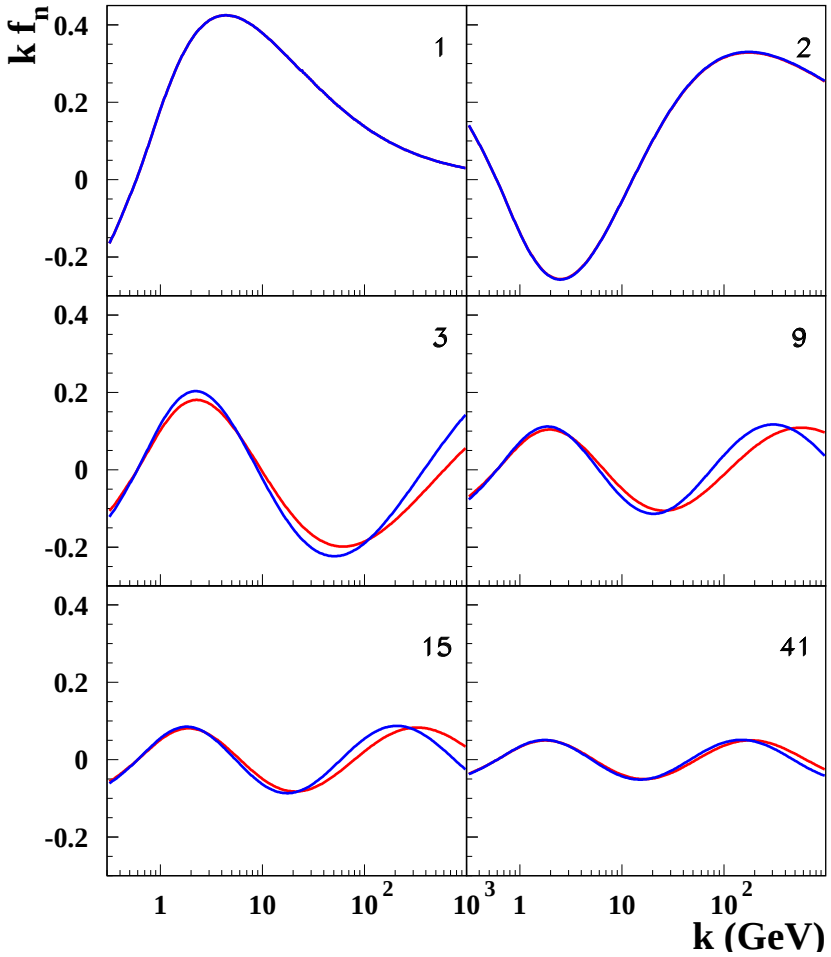

Figure 5: Comparison of a representative subset of eigenfunctions in the Standard Model (blue) and the SUSY model (red) computed with the same value of $\eta = 0$. The eigenvalue number is given in the upper right corner.

As explained in [1], since the eigenvalue tends to zero for large n, the form of the phase given by eq.(5.1) means that as a function of eigenvalue, ω, the phase has a cut singularity at $\omega = 0$, i.e.

$$\eta(\omega) \;=\; \left(\frac{a}{\omega}\right)^{\kappa} + b + c\omega + d\omega^2 + \cdots \tag{5.2}$$

This allows the generalization of eq.(5.1) by treating all the constants $a, b, c, d, \cdots$ in eq.(5.2) as free parameters. We have tested these parameterizations but find no improvement in the quality of the fit although we introduced more parameters; we therefore used the simple version of the phase condition, eq.(5.1), in all of our fits. In ref. [1] we fixed the value of the parameter η_0, which represents a total range of the η variation. In the present evaluation, since we have to perform many more fits, we prefer to treat it as a free parameter, to assure a bias free evaluation of all cases. Therefore we use in the fits the 3 parameters of eq.(5.1) and the 2 parameters from the proton impact factor. For the impact factor we take the parameterization

$$\Phi_p(k) \;=\; Ak^2 e^{-bk^2}, \tag{5.3}$$

as in ref. [1]. The fits were performed using the HERA data [2] with $x < 0.01$ and $Q^2 > 8$ GeV^2 or $Q^2 > 4$ GeV^2.

As in [1] we find that there is an significant improvement of χ^2/N_{df} in the $Q^2 > 8$ GeV^2 region due to various higher order effects, such as the NLO contribution to the photon impact factor and possibly also the proximity of the saturation region. In this region we have a total of 108 data points and a total of 5 parameters - so the number of degrees of freedom is $N_{df} = 103$. We therefore consider the $Q^2 > 8$ GeV^2 region as our main investigation region and use the $Q^2 > 4$ GeV^2 as a cross check.

We investigated the fit quality as a function of the maximal number of eigenfunctions, n_{max}. In contrast to the result of the analysis described in [1], we found that in the supersymmetric analysis the best fit can be obtained with a somewhat smaller number of eigenfunctions; only 100 (rather than 120) eigenfunctions are required to obtain the best χ^2. For the Standard Model the best fit is obtained with $n_{max} = 120$, but only with a small difference in the fit quality, $\chi^2 = 122.5(100)$ and $\chi^2 = 120.1(120)$.

In Table 1 we show our fits for various SUSY thresholds as well as the Standard Model. Let us first note that the $\tilde{k}_0$ values obtained in the unbiased fit, $\tilde{k}_0 \sim 275$ MeV, are close to Λ_{QCD}. At the same time the value of b implies that the proton impact factor peaks around Λ_{QCD}, as it should be in the self consistent description. This together with the relatively low χ^2's of all fits confirms the success of our construction of the infrared boundary.

The quality of the fits shows a clear preference of the evaluation with SUSY effects; the fit for the Standard model is worse than the fits with SUSY thresholds larger than 3 TeV. A SUSY threshold of 3 TeV, which is close to the reach of LHC also gives a worse fit. On the other hand for a SUSY threshold in the region of 10 - 15 TeV, the quality of the fit is the best, but that for significantly larger SUSY thresholds the fit quality worsens again.

Although the overal quality of the fit for all data with $Q^2 > 4\,\mathrm{GeV}^2$ is significantly worse, for reasons outlined above, the preference for N=1 SUSY with the threshold region of 10-15 TeV is also seen from a fit to the $Q^2 > 4$ GeV^2 data. In this Q^2 region there are 128

SUSY Scale (TeV)	χ^2	κ	$\tilde{k}_0$ (GeV)	η_0	A	b
3	125.7	0.555	0.288	-0.87	201.2	10.6
6	114.1	0.575	0.279	-0.880	464.8	15.0
10	109.9	0.565	0.275	-0.860	720.1	17.7
15	110.1	0.555	0.279	-0.860	882.2	18.6
30	117.8	0.582	0.278	-0.870	561.6	16.2
50	114.9	0.580	0.279	-0.870	627.4	16.8
90	114.8	0.580	0.279	-0.870	700.2	17.5
∞	122.5	0.600	0.274	-0.800	813.1	17.5

Table 1: Fits for N=1 SUSY at different scales. The bottom row corresponds to the Standard Model. All fits are performed with $n_{max} = 100$.

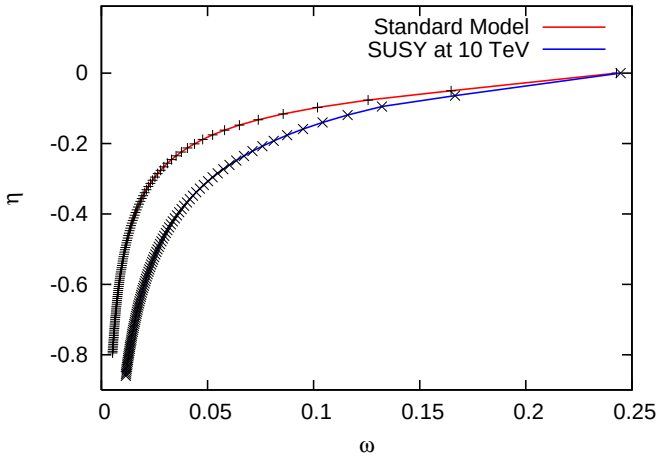

Figure 6: The eigenvalues and infrared phases for the Standard Model and N=1 SUSY at 10 TeV, as determined at $k = \tilde{k}_0$.

points and the χ^2 's of the best fits are 184.3 (3TeV), 164.5 (6TeV), 155.6 (10TeV), 152.6 (15TeV), 169.7 (30TeV), 164.7 (50TeV), 164.3 (90TeV). The best χ^2 for Standard Model is 169.7. The values of the fit parameters are similar to the values shown in Table 1, for the $Q^2 > 8$ GeV^2 region.

The consistency of the fit results and a clear χ^2 preference of the SUSY fits (with a scale above 3 TeV) over that for the Standard Model indicates that supersymmetry improves the data description and suggests that some new physics similar to $N = 1$ SUSY is present in the 10 - 15 TeV region.

6 Infrared Boundary: $\eta - \omega$ relation

The infrared boundary condition that leads to a discrete spectrum can be expressed as the ansatz that the phase at some infrared transverse momentum, $\tilde{k}_0$, is a fixed function, $\eta(\omega)$ of the eigenvalue ω, of the form given by eq.(5.2), imposed by the infrared properties of QCD. The discrete pomeron spectrum is driven by this function. Therefore, in Fig. 6 we show the values of the eigenvalues ω_n and the infrared phases η_n (in units of π) both for the Standard Model and $N = 1$ SUSY at a threshold of 10 TeV. The numerical values of the parameters on the RHS of eq.(5.2) turn out to be substantially different in the two cases. This function constitutes the infrared boundary conditions on the eigenvalues of the BFKL kernel. As explained above the eigenvalues are somewhat larger for the SUSY model, but both of these functions have a cut at $\omega = 0$, the order of the cut singularity being a little less in the case of the SUSY model (the dip is not so steep).

As was discussed in ref. [1] the appearance of the singularity in the $\eta-\omega$ relation indicates that some important contribution to the perturbative expansion at very large transverse momenta is missing. Therefore it is interesting to observe that the introduction of SUSY softens somewhat the observed singularity (κ is reduced from 0.6 to 0.56) and at the same time reduces the number of eigenfunctions required - it is a step towards a description of data using only few discrete pomerons. This could also indicate that there exist other, even stronger symmetries at very high energies, which are missing in the present evaluation, and which are responsible for the remaining singularity of the phase $\eta(\omega)$.

7 Summary

In our previous paper [1] we have shown that DPS gives a very good description of the low-x HERA data and it was suggested that this fit may have sensitivity to BSM physics. This proposed sensitivity emerged from the fact that the higher eigenfunctions have support over a very large range (see eq. (2.5)), extending from the infrared region to way above the threshold for any new physics and that through the required phase-matching process, the low energy behaviour of these eigenfunctions depends on their high-energy behaviour.

In this paper, we have shown that this is indeed the case. The introduction of N=1 SUSY at some threshold alters the value of the β-function and hence the rate of the running of the coupling. Furthermore there are contributions to the NLO characteristic function of the BFKL equation from the SUSY partners. Since the properties of the discrete pomeron are determined from a combination of the running coupling and the characteristic function, the eigenfunctions of the BFKL kernel are significantly affected by the introduction of SUSY. Notwithstanding the fact that the proposed SUSY scale is considerably above the scale probed at HERA, the altered high-energy behaviour of the eigenfunctions feeds into the low-energy, as well as generating a somewhat different spectrum of eigenvalues.

The discrete spectrum depends on the treatment of the infrared boundary condition, which is now more involved due to the fact that we are using the two-loop α_s running, instead of one-loop, as in [1]. Constructing this boundary we took the most conservative

approach of using perturbative QCD as a guideline at every step. Our previous paper was devoted to the task of finding the relation between the eigenfunction number and the phase of the eigenfunction oscillations which is essentially of the non-perturbative origin. Notwithstanding the substantial differences between the eigenfunctions with and without SUSY, we find here that the best fit is obtained using the same form of this dependence as was used in that paper, although other forms for this dependence were attempted without improving the fit quality.

Together, the different spectrum of eigenvalues and the different shapes of the eigenfunctions in turn affect the parameters of the fit to data and also the quality of the fit. The main result of this paper is that if the SUSY threshold is introduced at 10 -15 TeV, the fit was significantly better than that of the Standard Model ($\chi^2 = 110$ as compared to $\chi^2 = 122$ for 108 points and 103 degrees of freedom, i.e $\chi^2/N_{df} = 1.06$ vs 1.18). On the other hand, the introduction of SUSY at the threshold of 3 TeV, just within the reach of LHC, generates a fit which is no better than the fit obtained from the Standard Model.

It is pertinent to emphasize the qualitative difference between the fit obtained here and the usual DGLAP fit [10]. Over the low-x region, this DGLAP fit obtains a slightly better value of χ^2 per degree of freedom ($\chi^2/N_{df} \sim 0.95$). However, the DGLAP parameterization is designed to cover the entire range of x, whereas ours is only valid for sufficiently low-x where an expansion in $\ln(1/x)$ is valid. The improved quality of the fit of [10] is likely to be due to the terms with positive powers of x that are present in that fit. The important qualitative difference between the two fitting procedures is that the parameters obtained in the DGLAP approach are unaffected by any new physics at high-energy thresholds - their prediction for the structure functions would remain unchanged until the threshold (in Q^2) for new physics were reached. On the other hand, as we have emphasized in this paper, the values of our parameters are affected by new physics thresholds and consequently the Q^2 evolution above the fit region will always be affected by such new physics. This considerably stronger predictive power of the BFKL equation is not only due to the fact that it is a different type of evolution equation, but also that it describes the dynamics of the gluon-gluon interaction which (after accounting for the infrared boundary conditions) produces the two-gluon quasi-bound states with a non trivial spectrum of singularities in the j-plane.

The method described in this paper opens a new possibility to use high precision experiment to search for new physics at energy scales considerably larger than the scales at which the experiments are performed. It can be applied to any low-x process which was measured with comparable accuracy to the HERA F_2 data, like the Drell-Yan or W and Z production at LHC. The application of this method to LHC data could lead to higher sensitivity due to substantially higher scales involved. The discrete pomeron solution provides a unique tool for such an investigation owing to the fact that the construction of the eigenfunctions is based on the quantum mechanical approach in which the extremely high energy (up to the Planck scale) and low energy behaviour of its wave functions are intimately connected.

Acknowledgements:
The authors are grateful to the Marie Curie Foundation for an IRSES grant, LOWXGLUE Project 22498, which has facilitated this collaboration. Two of us (HK and DAR) wish to

thank the St. Petersburg Nuclear Physics Institute for its hospitality while this work was carried out.

References

[1] H. Kowalski, L.N. Lipatov, D. A. Ross, and G. Watt Eur. Phys. J **C70** (2010) 983; Nucl. Phys **A854** (2011) 45

[2] F. D. Aaron *et al.* [H1 and ZEUS Collaborations], JHEP **1001** (2010) 109.

[3] I. I. Balitsky and L. N. Lipatov, Sov. J. Nucl. Phys. **28** (1978) 822; E. A. Kuraev, L. N. Lipatov and V. S. Fadin, Sov. Phys. JETP **44** (1976) 443; V. S. Fadin, E. A. Kuraev and L. N. Lipatov, Phys. Lett. B **60** (1975) 50.

[4] V. S. Fadin and L. N. Lipatov, Phys. Lett. B **429** (1998) 127;
M. Ciafaloni and G. Camici, Phys. Lett. B **430** (1998) 349.

[5] G. P. Salam, JHEP **9807** (1998) 019.

[6] J. Ellis, H. Kowalski and D. A. Ross, Phys. Lett. B **668** (2008) 51.

[7] L. N. Lipatov, Sov. Phys. JETP **63** (1986) 904.

[8] C. Adloff *et al.* [H1 Collaboration], Eur. Phys. J. C **21** (2001) 33;
S. Chekanov *et al.* [ZEUS Collaboration], Eur. Phys. J. C **21** (2001) 443.

[9] A. V. Kotikov and L. N. Lipatov, Nucl. Phys. B **582** (2000) 19;
Nucl. Phys. B **661** (2003) 19.

[10] A. D. Martin, W. J. Stirling, R. S. Thorne and G. Watt, Eur. Phys. J. C **63** (2009) 189.